

## Three Guest-Including Coordination Solids from a Single Crystallization: A Discrete Cage and Open-Channel Networks from 1-D Ladders and 1-D Ribbons

Amir H. Mahmoudkhani and George K. H. Shimizu\*

Department of Chemistry, University of Calgary, Calgary, Alberta T2N 1N4, Canada

Received August 10, 2006

A study of the coordination assemblies that result from the complexation of 1,3,5-tri(4-sulfophenyl)benzene,  $L^{3-}$ , with copper(II) in the presence of pyridine is presented. The present results offer some insights into the subtleties of designing coordination polymers and open-channel solids. From an initial crystallization, three different single crystalline solids, **1–3**, are obtained. Compounds **1** and **2** are Cu pyridyl complexes of the trianionic form of the ligand whereas compound **3** is a Cu pyridyl complex of the monoprotonated form,  $HL^{2-}$ . Compound **1** is a discrete cage complex. Compound **2** is a 1-D ladder structure that has open channels, and compound **3** is a 1-D ribbon structure that assembles into open channels. All three complexes form from the same crystallization in a ratio of 90:9:1, and all three have the same Cu coordination sphere. The exact ratio of products can be altered by varying the Cu counterion or by the addition of methanol. Addition of hexamethylenetetramine results in the exclusive formation of a different network, **4**, which is structurally almost identical to the minor product **3**. Single-crystal structures of all four solids are presented along with thermal analysis and IR data for the major products. A number of insights into formation of coordination assemblies are obtained. Compound **3** is discussed as an intermediate to **2**, and compounds **3** and **4** offer a design paradigm for the formation of open-channel solids from 1-D building blocks.

### Introduction

The use of the coordinate-covalent bond has been extensively studied in the formation of both discrete and infinite metal–organic assemblies. From a basic supramolecular perspective, the use of coordinate-covalent bonding versus covalent bonding allows for a degree of reversibility and, hence, “error checking” in the assembly process.<sup>1</sup> This is manifested typically as high degrees of order (i.e., crystallinity) in coordination assemblies. For discrete systems, the inherent higher solubility of intermediates and product would be expected to enable the self-assembly process to continue until the minimized structure is attained.<sup>2</sup> For infinite solids, metastable phases can precipitate as intermediate structures, capable of further nucleating their own growth, resulting in the observation of different polymorphs or supramolecular isomers.<sup>3</sup>

With regards to both the self-assembly of discrete polyhedra and the formation of infinite coordination frameworks,

the inclusion of guest molecules is a fundamental point of interest as it suggests accessibility of the interior of the solid for potential applications (e.g., sorption, sensing, catalysis).<sup>4</sup> Formation of solids containing solvated cavities is typically enthalpically disfavored as building blocks will tend to arrange in a manner to efficiently fill space. Thus, in general, the greater the guest component in a solid, the more difficult its preparation and the more challenging the design aspect becomes.

We<sup>5</sup> and others<sup>6</sup> have been interested in the ability of the sulfonate group to form functional coordination frameworks. The sulfonate group is generally regarded as weakly ligating,

- (2) (a) Fujita, M. *Chem. Soc. Rev.* **1998**, 27, 417. (b) Mukherjee, P. S.; Das, N.; Kryschenko, Y. K.; Arif, A. M.; Stang, P. J. *J. Am. Chem. Soc.* **2004**, 126, 2465. (c) Atwood, J. L.; Szumna, A. *J. Am. Chem. Soc.* **2002**, 124, 10646. (d) Ovchinnikov, M. V.; Holliday, B. J.; Mirkin, C. A.; Zakharov, L. N.; Rheingold, A. L. *Proc. Natl. Acad. Sci. U.S.A.* **2002**, 99, 4927. (e) Hamilton, T. D.; Papaefstathiou, G. S.; MacGillivray, L. R. *J. Am. Chem. Soc.* **2002**, 124, 11606. (f) Yoshizawa, M.; Fujita, M. *Pure Appl. Chem.* **2005**, 77, 1107. (g) Moulton, B.; Lu, J.; Mondal, A.; Zaworotko, M. J. *Chem. Commun.* **2001**, 863. (h) Eddaoudi, M.; Kim, J.; Wachter, J. B.; Chae, H. K.; O’Keeffe, M.; Yaghi, O. M. *J. Am. Chem. Soc.* **2001**, 123, 4368.

\* To whom correspondence should be addressed. Tel: 1-403-220-5347. Fax: 1-403-289-9488. E-mail: gshimizu@ucalgary.ca.

(1) (a) Lehn, J. M. *Pure Appl. Chem.* **1994**, 66, 1961. (b) Lehn, J. M. *Rep. Prog. Phys.* **2004**, 67, 249.

even within the domain of coordinate-covalent bonding. The general trend in bonding is that, for harder ions, sulfonate ions tend not to compete with other donors. For example, from water, hard metal cations will often remain fully hydrated.<sup>7</sup> For softer ions, with most examples being for silver(I)<sup>8</sup> and heavier alkaline earth ions,<sup>9</sup> complexes with highly ligated metal ions and multiply bridging RSO<sub>3</sub> groups can be observed even in aqueous solutions. Copper(II) has also been examined with sulfonate ions, and like hard cations, it will form a solvent-separated ion pair in water.<sup>10</sup> However, in the presence of amine or pyridine ligands, a common coordination motif adopted by copper(II) is a tetragonally elongated octahedron with equatorial sites occupied by the N donors and the two axial sites filled by sulfonate groups.<sup>11</sup>

Coupling this coordination chemistry with appropriately chosen organic cores can result in infinite frameworks which demonstrate open-channel structures and/or can indeed demonstrate some guest sorption properties from both the liquid and gas phases.

In this work, we present a system which illustrates both the potential and the difficulties of designing open framework coordination solids. Three sulfonic acid groups were anchored to a rigid trigonally symmetric core in the triacid of 1,3,5-tri(4-sulfophenyl)benzene, H<sub>3</sub>L. This ligand was then complexed to copper(II) in the presence of pyridine resulting in the formation of three different assemblies, two being infinite frameworks and the other being a discrete structure. The discrete complex, [Cu<sub>3</sub>L<sub>2</sub>(py)<sub>12</sub>]·pyridine, **1**, forms a neutral cage structure where two molecules of L are oriented by three Cu centers at an ideal distance to trap aromatics, in this case, a guest pyridine molecule. This solid represents a pseudo polymorph of one of the infinite assemblies, {[Cu<sub>3</sub>L<sub>2</sub>(py)<sub>12</sub>(pyridine)·xH<sub>2</sub>O]<sub>∞</sub>}, **2**. Compound **2** forms a 1-D ladder structure where the trigonal organic ligand acts as the branch point for each rung. The channels between rungs of the ladder measure ~14 × 22 Å and are filled with disordered guest-solvent molecules. The final structure, {[CuHL(py)<sub>4</sub>](pyridine)·xH<sub>2</sub>O]<sub>∞</sub>}, **3**, has a different stoichiometry as only two of the three sulfonic acid groups on H<sub>3</sub>L are deprotonated. Compound **3** possesses a 1-D ribbon structure, with pendent organic groups. These ribbons further assemble noncovalently in the remaining two dimensions to form a network with channels (> 15 Å) permeating it in one dimension. This observation of large guest-filled channels in a solid from 1-D building blocks is unusual, and an explanation and future design prospectus of this motif is proposed in this work. Despite having very different overall structural motifs, compounds **1–3** are all guest-including solids, all have copper centers with the same coordination sphere, and all three are obtained from the same recrystallization in a relative 1/2/3 ratio of 90:9:1. Compound **3** represents a likely intermediate of **2** as will be explained. In a separate experiment, we also show that by addition of hexamethyl-

- (3) (a) Moulton, B.; Zaworotko, M. J. *Chem. Rev.* **2001**, *101*, 1629. (b) Huang, X. C.; Zhang, J. P.; Chen, X. M. *J. Am. Chem. Soc.* **2004**, *126*, 13218. (c) Gale, P. A.; Light, M. E.; Quesada, R. *Chem. Commun.* **2005**, 5864. (d) Lee, I. S.; Shin, D. M.; Chung, Y. K. *Chem.—Eur. J.* **2004**, *10*, 3158. (e) Masaoka, S.; Tanaka, D.; Nakanishi, Y.; Kitagawa, S. *Angew. Chem., Int. Ed.* **2004**, *43*, 2530. (f) Ring, D. J.; Aragoni, M. C.; Champness, N. R.; Wilson, C. *CrystEngComm.* **2005**, *7*, 621. (g) Zhang, J. P.; Lin, Y. Y.; Huang, X. C.; Chen, X. M. *Dalton Trans.* **2005**, 3681. (h) Saha, B. K.; Jetti, R. K. R.; Reddy, L. S.; Aitipamula, S.; Nangia, A. *Cryst. Growth Des.* **2005**, *5*, 887. (i) Zhang, J. P.; Lin, Y. Y.; Chen, X. M. *Chem. Commun.* **2005**, 2232. (j) Horikoshi, R.; Mochida, T.; Kurihara, M.; Mikuriya, M. *Cryst. Growth Des.* **2005**, *5*, 243. (k) Mezei, G.; Baran, P.; Raptis, R. G. *Angew. Chem., Int. Ed.* **2004**, *43*, 574. (l) Su, C. Y.; Gofarth, A. M.; Smith, M. D.; zur Loye, H. C. *Inorg. Chem.* **2003**, *42*, 5685. (m) Zimmer, B.; Bulach, V.; Hosseini, M. W.; De Cian, A.; Kyritsaka, N. *Eur. J. Inorg. Chem.* **2002**, 3079. (n) Soldatov, D. V.; Henegouwen, A. T.; Enright, G. D.; Ratcliffe, C. I.; Ripmeester, J. A. *Inorg. Chem.* **2001**, *40*, 1626. (o) Jiang, L.; Lu, T. B.; Feng, X. L. *Inorg. Chem.* **2005**, *44*, 7056. (p) Soldatov, D. V.; Zanina, A. S.; Enright, G. D.; Ratcliffe, C. I.; Ripmeester, J. A. *Cryst. Growth Des.* **2003**, *3*, 1005.
- (4) (a) Rowsell, J. L. C.; Yaghi, O. M. *J. Am. Chem. Soc.* **2006**, *128*, 1304. (b) Matsuda, R.; Kitaura, R.; Kitagawa, S.; Kubota, Y.; Belosludov, R. V.; Kobayashi, T. C.; Sakamoto, H.; Chiba, T.; Takata, M.; Kawazoe, Y.; Mita, Y. *Nature* **2005**, *436*, 238. (c) Eddaoudi, M.; Kim, J.; Rosi, N.; Vodak, D.; Wachter, J.; O’Keeffe, M.; Yaghi, O. M. *Science* **2002**, *295*, 469. (d) MasPOCH, D.; Ruiz-Molina, D.; Wurst, K.; Domingo, N.; Cavallini, M.; Biscarini, F.; Tejada, J.; Rovira, C.; Veciana, J. *Nat. Mater.* **2003**, *2*, 190. (e) Seo, J. S.; Whang, D.; Lee, H.; Jun, S. I.; Oh, J.; Jeon, Y. J.; Kim, K. *Nature* **2000**, *404*, 982. (f) Soldatov, D. V.; Ripmeester, J. A. *Chem. Mater.* **2000**, *12*, 1827. (g) Tabares, L. C.; Navarro, J. A. R.; Salas, J. M. *J. Am. Chem. Soc.* **2001**, *123*, 383. (h) Fletcher, A. J.; Cussen, E. J.; Prior, T. J.; Rosseinsky, M. J.; Kepert, C. J.; Thomas, K. M. *J. Am. Chem. Soc.* **2001**, *123*, 10001.
- (5) (a) Côté, A. P.; Shimizu, G. K. H. *Coord. Chem. Rev.* **2003**, *245*, 49. (b) Shimizu, G. K. H. *J. Solid State Chem.* **2005**, *178*, 2519.
- (6) (a) Cai, J. W. *Coord. Chem. Rev.* **2004**, *248*, 1061. (b) Chen, C. H.; Cai, J. W.; Liao, C. Z.; Feng, X. L.; Chen, X. M.; Ng, S. W. *Inorg. Chem.* **2002**, *41*, 4967. (c) Cai, J. W.; Zhou, J. S.; Lin, M. L. *J. Mater. Chem.* **2003**, *13*, 1806. (d) Atwood, J. L.; Barbour, L. J.; Hardie, M. J.; Raston, C. L. *Coord. Chem. Rev.* **2001**, *222*, 3. (e) Kennedy, A. R.; Hughes, M. P.; Monaghan, M. L.; Staunton, E.; Teat, S. J.; Smith, W. E. *J. Chem. Soc., Dalton Trans.* **2001**, 2199. (f) Cai, J. W.; Chen, C. H.; Feng, X. L.; Liao, C. Z.; Chen, X. M. *J. Chem. Soc., Dalton Trans.* **2001**, 2370. (g) Liu, Y.; Su, J.; Li, W.; Wu, J. *Inorg. Chem.* **2005**, *44*, 3890. (h) Mezei, G.; Raptis, R. G. *New J. Chem.* **2003**, *27*, 1399. (i) Park, S. H.; Lee, C. E. *Chem. Commun.* **2003**, 1838. (j) Chandrasekhar, V.; Boomishankar, R.; Singh, S.; Steiner, A.; Zaccchini, S. *Organometallics* **2002**, *21*, 4575. (k) Kennedy, A. R.; Kirkhouse, J. B. A.; McCarney, K. M.; Puissegur, O.; Smith, W. E.; Staunton, E.; Teat, S. J.; Cherryman, J. C.; James, R. *Chem.—Eur. J.* **2004**, *10*, 4606. (l) Sun, Z. M.; Mao, J. G.; Sun, Y. Q.; Zeng, H. Y.; Clearfield, A. *Inorg. Chem.* **2004**, *43*, 336.
- (7) (a) Dalrymple, S. A.; Shimizu, G. K. H. *Supramol. Chem.* **2003**, *15*, 591. (b) Dalrymple, S. A.; Parvez, M.; Shimizu, G. K. H. *Chem. Commun.* **2001**, 2672. (c) Guo, Q. L.; Zhu, W. X.; Dong, S. J.; Ma, S. L.; Yan, X. *J. Mol. Struct.* **2003**, *650*, 159. (d) Chandrasekhar, V.; Boomishankar, R.; Singh, S.; Steiner, A.; Zaccchini, S. *Organometallics* **2002**, *21*, 4575. (e) Leonard, M. A.; Squattrito, P. J.; Dubey, S. N. *Acta Crystallogr., Sect. C* **1999**, *55*, 35.
- (8) (a) Côté, A. P.; Ferguson, M. J.; Khan, K. A.; Enright, G. D.; Kulynych, A. D.; Dalrymple, S. A.; Shimizu, G. K. H. *Inorg. Chem.* **2002**, *41*, 287. (b) Shimizu, G. K. H.; Enright, G. D.; Ratcliffe, C. I.; Rego, G. S.; Reid, J. L.; Ripmeester, J. A. *Chem. Mater.* **1998**, *10*, 3282. (c) Côté, A. P.; Shimizu, G. K. H. *Inorg. Chem.* **2004**, *43*, 6663. (d) Ma, J. F.; Yang, J.; Li, S. L.; Song, S. Y.; Zhang, H. J.; Wang, H. S.; Yang, K. Y. *Cryst. Growth Des.* **2005**, *5*, 807. (e) Li, F. F.; Ma, J. F.; Song, S. Y.; Yang, J.; Liu, Y. Y.; Su, Z. M. *Inorg. Chem.* **2005**, *44*, 9374. (f) Shimizu, G. K. H.; Enright, G. D.; Ratcliffe, C. I.; Preston, K. F.; Reid, J. L.; Ripmeester, J. A. *Chem. Commun.* **1999**, 1485. (g) May, L. J.; Shimizu, G. K. H. *Chem. Mater.* **2005**, *17*, 217. (h) Smith, G.; Cloutt, B. A.; Lynch, D. E.; Byriel, K. A.; Kennard, C. H. L. *Inorg. Chem.* **1998**, *37*, 3236. (i) Hoffart, D. J.; Dalrymple, S. A.; Shimizu, G. K. H. *Inorg. Chem.* **2005**, *44*, 8868. (j) Sun, D. F.; Cao, R.; Bi, W. H.; Li, X. J.; Wang, Y. Q.; Hong, M. C. *Eur. J. Inorg. Chem.* **2004**, *10*, 2144.
- (9) (a) Côté, A. P.; Shimizu, G. K. H. *Chem.—Eur. J.* **2003**, *9*, 5361. (b) Dalrymple, S. A.; Shimizu, G. K. H. *Chem.—Eur. J.* **2002**, *8*, 3010. (c) Liu, Y. F.; Su, J. C.; Li, W. H.; Wu, J. G. *Inorg. Chem.* **2005**, *44*, 3890. (d) Hoffart, D. J.; Côté, A. P.; Shimizu, G. K. H. *Inorg. Chem.* **2003**, *42*, 8603.
- (10) (a) Dalrymple, S. A.; Parvez, M.; Shimizu, G. K. H. *Inorg. Chem.* **2002**, *41*, 6986. (b) Sharma, R. P.; Sharma, R.; Bala, R.; Rychlewski, U.; Warzajtis, B. *J. Mol. Struct.* **2005**, *738*, 291.
- (11) Cai, J. W.; Chen, C. H.; Liao, C. Z.; Yao, J. H.; Hu, X. P.; Chen, X. M. *J. Chem. Soc., Dalton Trans.* **2001**, 1137.

**Table 1.** Crystal Data and Refinement Summaries for Compounds **1–4**

formula	C <sub>113</sub> H <sub>95</sub> Cu <sub>3</sub> N <sub>13</sub> O <sub>18</sub> S <sub>6</sub> [Cu <sub>3</sub> (L) <sub>2</sub> (py) <sub>12</sub> ]·py ( <b>1</b> )	C <sub>108</sub> H <sub>90</sub> Cu <sub>3</sub> N <sub>12</sub> O <sub>19</sub> S <sub>6</sub> [Cu <sub>3</sub> (L) <sub>2</sub> (py) <sub>12</sub> ]·(H <sub>2</sub> O) ( <b>2</b> )	C <sub>88</sub> H <sub>70</sub> Cu <sub>2</sub> N <sub>8</sub> O <sub>20</sub> S <sub>6</sub> [Cu <sub>2</sub> (HL) <sub>2</sub> (py) <sub>8</sub> ]·py·2H <sub>2</sub> O ( <b>3</b> )	C <sub>44</sub> H <sub>35</sub> Cu <sub>4</sub> O <sub>11.25</sub> S <sub>3</sub> [Cu <sub>2</sub> (HL) <sub>2</sub> (py) <sub>8</sub> ]·4.5H <sub>2</sub> O ( <b>4</b> )
fw	2306.0	2242.90	1878.96	1918.96
cryst syst	trigonal	triclinic	monoclinic	triclinic
space group	R $\bar{3}c$ (No. 167)	P $\bar{1}$ (No. 2)	Cc (No. 9)	P $\bar{1}$ (No. 2)
<i>a</i> (Å)	20.324(5)	10.510(2)	17.793(4)	17.1180(2)
<i>b</i> (Å)	20.324(5)	14.158(3)	39.817(8)	21.2660(3)
<i>c</i> (Å)	47.623(5)	21.748(4)	10.563(2)	21.8720(4)
$\alpha$ (deg)	90	108.91(3)	90	99.079(1)
$\beta$ (deg)	90	93.16(3)	112.07(3)	109.79(1)
$\gamma$ (deg)	120	90.43(3)	90	102.65(1)
<i>V</i> (Å <sup>3</sup> )	17 036(6)	3055.8(11)	6935(2)	7072.4(2)
<i>Z</i>	6	1	2	2
<i>D</i> <sub>calcd</sub> (g/cm <sup>3</sup> )	1.349	1.210	0.900	0.901
$\mu$ (mm <sup>-1</sup> )	0.737	0.682	0.445	0.438
$\lambda$ (Å)	0.71073	0.71073	0.71073	0.71073
data [ <i>I</i> > 2 $\sigma$ ( <i>I</i> )]/params	3462/226	9667/824	12 631/521	17 436/1038
GOF	1.170	1.043	1.112	1.472
final <i>R</i> indices [ <i>I</i> > 2 $\sigma$ ( <i>I</i> )]	R1 = 0.1096 wR2 = 0.3136	R1 = 0.0790 wR2 = 0.2233	R1 = 0.0902 wR2 = 0.2442	R1 = 0.134 wR2 = 0.345
final <i>R</i> indices (all data)	R1 = 0.1239 wR2 = 0.3288	R1 = 0.1113 wR2 = 0.2500	R1 = 0.1050 wR2 = 0.2640	R1 = 0.151 wR2 = 0.340

enetetramine as a template to the recrystallization mixture which yields the **1/2/3** mixture it is possible to obtain another network, **4**, {[CuHL(py)<sub>4</sub>] $\cdot$ xH<sub>2</sub>O}<sub>∞</sub>, as the major product. Compound **4**, although having different crystallographic parameters to those of **3**, has a nearly identical structure composed of 1-D ribbons assembling into an open-channel structure. Compound **1** has been the subject of a preliminary communication.<sup>12</sup>

## Experimental Section

**General Procedures and Instrumentation.** TGA/DSC analyses were performed on a Netzsch 449C simultaneous thermal analyzer under a dynamic N<sub>2</sub> atmosphere at a scan rate of 5 °C/min, with samples heated in pierced hermetically sealed pans. All chemicals were purchased from Aldrich Chemical Co. and used as received. IR spectra were recorded on a Nicolet Nexus 470.

**General X-ray Crystallography.** Crystals suitable for X-ray analysis were chosen under an optical microscope and quickly coated in oil before being mounted in a nylon loop and frozen under a stream of cryogenic nitrogen gas (−100 °C) for data collection. Standard graphite monochromated Mo K $\alpha$  radiation ( $\lambda$  = 0.71073 Å) was employed. Single-crystal X-ray data were collected on a Nonius Kappa CCD diffractometer using a data acquisition strategy determined from the HKL2001 suite of programs.<sup>13</sup> Likewise, data were processed and intensities were corrected for Lorentz and polarization effects and for absorption using this software. All structures were solved by direct methods using SHELXS-97<sup>14</sup> and refined on *F*<sup>2</sup> by full-matrix least-squares procedures with SHELXL-97. All non-hydrogen atoms were refined with anisotropic displacement parameters with the exception of disordered atoms. Hydrogen atoms were included in calculated positions with isotropic displacement parameters 1.5 times the isotropic equivalent of their carrier atoms. For compounds **3** and **4**, owing to the high degree of disordered solvent, the SQUEEZE routine of Platon was employed.<sup>15</sup> Final atomic coordinates, thermal parameters, and com-

plete listing of bond lengths and angles are deposited, available from the Cambridge Crystallographic Data Centre. Pertinent structure refinement data for **1–4** are in Table 1.

**Preparation of the Triacid of 1,3,5-Tri(4-sulfonophenyl)-benzene, H<sub>3</sub>L:** 1,3,5-Triphenylbenzene (1.00 g, 3.26 mmol) was dissolved in dry CH<sub>2</sub>Cl<sub>2</sub> (100 mL) in a 250 mL flask under an atmosphere of dry nitrogen gas. ClSO<sub>3</sub>H (2 mL, 29.3 mmol) was added dropwise to the above solution while it was stirred. Then, the mixture was brought to reflux for 10 h. The product was hydrolyzed using water (10 mL). A white precipitate formed immediately and was then separated by vacuum filtration, oven dried, and placed in a desiccator. Yield: 1.48 g, 2.70 mmol (83%). <sup>1</sup>H NMR (200.13 MHz, D<sub>2</sub>O): 7.81, 7.85, 7.88, 7.93 ppm. <sup>13</sup>C NMR (50.33 MHz, D<sub>2</sub>O): 123.64, 125.29, 126.10, 126.46, 138.58, 140.77, 141.33 ppm. Treatment with NaHCO<sub>3</sub> (aq), provided the sodium salt. IR (KBr, cm<sup>-1</sup>): 3456 (s, br), 3056 (w), 1630 (m), 1595 (m), 1565 (w), 1504 (w), 1443 (w), 1391 (w), 1191 (s), 1134 (s), 1039 (s), 1000 (s), 882 (w), 834 (m) 704 (s), 621 (m), 565 (m), 448 (w).

**Synthesis of Complexes 1–3:** The following preparation, carried through undisturbed, will give compounds **1**, **2**, and **3** in a relative ratio of 90:9:1. In replicate preparations, crystals were removed for study. Cu(NO<sub>3</sub>)<sub>2</sub>·2.5H<sub>2</sub>O (0.11 g, 0.487 mmol) and Na<sub>3</sub>L (0.20 g, 0.325 mmol) were each dissolved in water (3 mL). After mixing of the solution, the light blue solution was heated gently to about 60 °C, to the point at which the solvent was evaporated to half of its original volume. The remaining solution was kept in a closed container, and pyridine was vapor-diffused in. The solution turned dark blue, and in a period of 4–6 days, dark blue cubelike crystals of trigonal compound **1**, [Cu<sub>3</sub>L<sub>2</sub>(py)<sub>12</sub>]·pyridine, were formed. (Yield after 6 days: 50–60%). Upon standing for any longer time period, crystals of both **2** and **3** gradually appear, although it is difficult to distinguish them conclusively without mechanically separating the crystals and performing a unit cell determination. Figure 1 shows the habits and relative amounts of **1** and the other two crystals obtained from a typical crystallization. Anal. Calcd: C, 58.86; H, 4.15; N, 7.90. Found: C, 58.36; H, 4.17; N, 8.32. IR (KBr pellet, cm<sup>-1</sup>): 3473 (w, br), 3117 (w), 3096 (w), 3072 (w), 3049 (w), 3030 (w), 3008 (w), 1608 (m), 1594 (sh), 1492 (w), 1449 (s), 1382 (w), 1236 (s), 1221 (sh), 1181 (s), 1153 (sh), 1124 (s), 1073 (m), 1031 (s), 1006 (s), 848 (sh), 836 (m), 761 (m), 706 (vs),

(12) Mahmoudkhani, A. M.; Côté, A. P.; Shimizu, G. K. H. *Chem. Commun.* **2004**, 2678.

(13) Otwinoski, Z.; Minor, W. In *Methods in Enzymology*; Carter, C. W., Jr., Sweet, R. M., Eds.; Pergamon Press: New York, 1997; Vol 273, p. 307.

(14) Sheldrick, G. M. *SHELX-97 Program for X-ray Crystal Structure Refinement*; University of Göttingen: Göttingen, Germany, 1997.

(15) Spek, A. L. *J. Appl. Cryst.* **2003**, 36, 7.

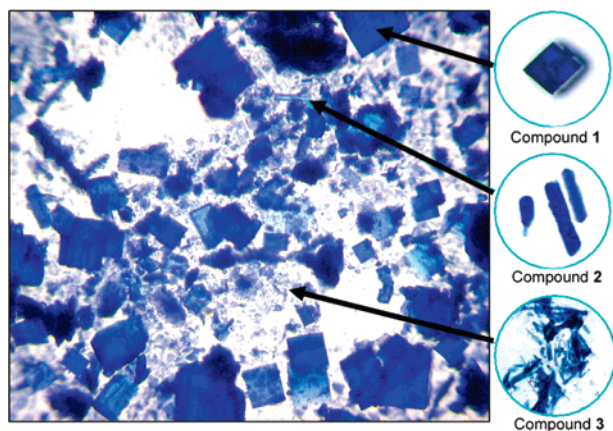


**Figure 1.** A typical crystallization of 1–3. The insets show the habits of each respective compound whereas the large figure shows their relative distribution in the bulk sample.

642 (w), 616 (s), 572 (m), 548 (w), 439 (w). Far-IR (CsI,  $\text{cm}^{-1}$ ): 436 (w), 389 (w). After 7 days, blue needlelike crystals formed, which were isolated and identified as triclinic compound 2,  $[\text{Cu}_3\text{L}_2(\text{py})_{12}(\text{pyridine}) \cdot x\text{H}_2\text{O}]$ . This second phase continued to grow with the concomitant appearance of a third phase observed after roughly 9 days as blue prismatic crystals. This was identified as the monoclinic compound 3,  $[\text{CuHL}(\text{py})_4](\text{pyridine}) \cdot x\text{H}_2\text{O}$ . Single crystals of 2 and 3 were mechanically separated from the mixture. These are present in small amounts, desolvate rapidly, and require an initial unit cell determination to confirm their identity. For these reasons, bulk quantities of 2 and 3 were not attainable.

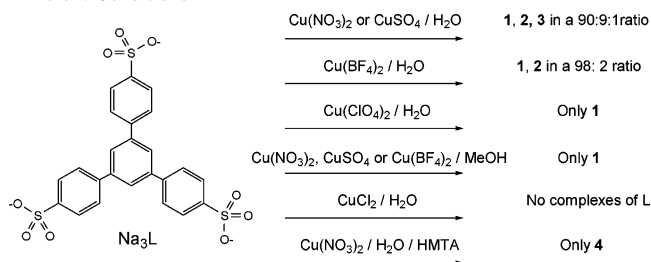
**Varying the Anion/Solvent in the  $\text{Cu}^{2+}$  Salt for 1–3:** The employment of analogous conditions to those above, with  $\text{CuSO}_4 \cdot 5\text{H}_2\text{O}$  in place of the nitrate salt, resulted in a similar 90:9:1 distribution of compounds 1/2/3. The use of  $\text{Cu}(\text{BF}_4)_2 \cdot \text{H}_2\text{O}$  in place of the nitrate salt resulted in the observation of only compounds 1 and 2 in a 98:2 ratio. Using  $\text{Cu}(\text{ClO}_4)_2 \cdot 6\text{H}_2\text{O}$  gave exclusively compound 1. With  $\text{CuCl}_2 \cdot 2\text{H}_2\text{O}$ , no solid corresponding to a complex of L was obtained. The addition of MeOH (0.5–1.0 mL) to any of the crystallizations above employing the  $\text{NO}_3^-$ ,  $\text{SO}_4^{2-}$ , or  $\text{BF}_4^-$  salts resulted in the formation of solely compound 1.

**Synthesis of Complex 4:**  $\text{Cu}(\text{NO}_3)_2 \cdot \text{H}_2\text{O}$  (28 mg, 0.12 mmol) and  $\text{Na}_3\text{L}$  (50 mg, 0.08 mmol) were dissolved in distilled water (5 mL). Hexamethylenetetramine (1.1 mg, 0.008 mmol) was added to the above solution, and the mixture was stirred for 30 min. The solution was transferred to a vial and stored over pyridine in a sealed container. The light colored solution turned to dark blue after one week by the diffusion of pyridine. Dark blue parallelepiped crystals were formed over a period of 4 months and were separated from the light blue-green mother liquor. (Yield after 4 months: 70–80%.) Anal. Calcd: C, 57.16; H, 3.92; N, 6.06. Found: C, 55.52; H, 3.60; N, 5.99. IR (KBr pellet,  $\text{cm}^{-1}$ ): 3456 (m, br), 3113 (w), 3056 (w), 1634 (w), 1604 (m), 1593 (sh), 1491 (w), 1447 (m), 1378 (w), 1217 (s), 1187 (s), 1121 (s), 1074 (m), 1034 (s), 1004 (s), 830 (m), 760 (m), 704 (s), 643 (w), 613 (s), 586 (sh), 569 (m), 547 (sh), 439 (w).

## Results

Three guest-including solids, 1–3, one discrete complex and two infinite frameworks, form from a single recrystallization (Figure 1). The compounds are initially distinguishable by their crystal morphology, then by their crystallographic symmetry, and finally by their solid-state structures. A fourth related compound, 4, with identical components

**Scheme 1.** Products of  $\text{Na}_3\text{L}$  Complexation with  $\text{Cu}^{2+}$  under Different Conditions



can be isolated from a different preparation. Compound 1 formed blocklike crystals which possessed trigonal symmetry. Compound 1 formed a discrete cage on the molecular level as will be described, with the other structures, in the ensuing section. Compound 2 had a needlelike crystal habit and possessed triclinic symmetry. The network formed by this complex can be described as a 1-D ladder structure with guests between the rungs of the ladder. Compound 3 formed prismatic crystals with monoclinic symmetry. The structure of this solid was that of 1-D ribbons which self-assembled into a large open-channel network. The exact ratios of the three products varied with conditions, but compound 1 always nucleated first and the relative yields of the three solids were always  $1 \gg 2 > 3$ . Interestingly, if hexamethylenetetramine is added to the preparation, a new crystalline product, 4, which is structurally very similar to the minor product 3, is obtained as the sole crystalline product. More detail on the factors influencing the preparation is presented after the structural descriptions. A summary of the preparative aspects of this work is summarized in Scheme 1.

**Single-Crystal Structure of Compound 1.** Compound 1,  $[\text{Cu}_3\text{L}_2(\text{py})_{12}] \cdot \text{pyridine}$ , is observed as a discrete cage structure composed of two molecules of L bridged by three Jahn–Teller distorted  $[\text{Cu}(\text{py})_4]^{2+}$  units (Figure 2a). The pyridine ligands occupy the equatorial sites on the  $\text{Cu}^{2+}$  ions ( $\text{Cu}-\text{N}1 = 2.023(3)$ ,  $\text{Cu}-\text{N}2 = 2.033(3)$  Å) with the sulfonate oxygen atoms coordinated axially ( $\text{Cu}-\text{O}2 = 2.461(3)$  Å). The axial ligation of sulfonates with  $\text{Cu}^{2+}$  and N donors is frequently observed. In this case, this is quite relevant as it situates the two molecules of L at a distance of 7.679 Å as measured by the interligand S–S distances. This is a nearly ideal value for  $\pi$ -stacking interactions with an aromatic ring, and indeed, a guest molecule of pyridine is observed in the cage. The guest pyridine forms weak face-to-face  $\pi$  interactions with the two ligand molecules (mean plane distance =  $2 \times 4.059 = 8.118$  Å). Laterally, there are no significant edge-to-face  $\pi$  interactions with the six inward-directed pyridine ligands as the shortest intermolecular C–C distance is  $> 3.9$  Å. The guest pyridine molecule is rotationally disordered over three sites. This is not unexpected given the relatively weak contacts with the surrounding ligated pyridine molecules. The two L molecules which form the top and bottom of the cage are perfectly eclipsed as shown in Figure 2b. The Jahn–Teller distortion is very important as, in a perfect octahedron, axially ligated  $\text{SO}_3$  groups and therefore the L ligands would lay 0.8–0.9 Å closer. This decrease in the cavity size is more than sufficient to prevent inclusion of aromatic guests.

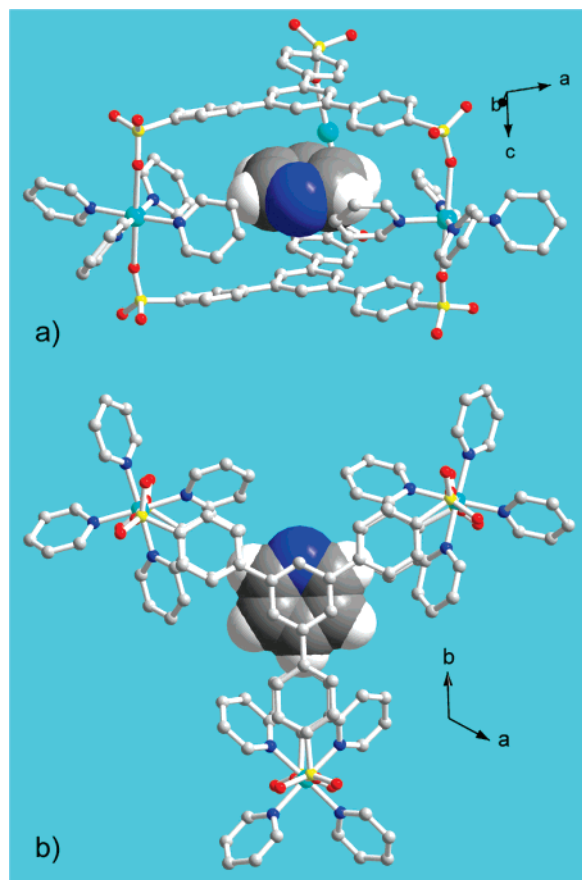


**Figure 2.** Single-crystal structure of compound **1**. (a) View of the cage showing the guest in a space-filling depiction. (b) Top view of the cage showing the eclipsed structure. H atoms and pyridine ligands on the rear Cu have been removed for clarity.

A range of weaker interactions further stabilizes compound **1**. With respect to the cage, interactions exist between the acidic  $\alpha$ -hydrogen atoms of the coordinated pyridine molecules and the axially ligated sulfonate oxygen atom ( $O\cdots H = 2.567\text{--}2.940\text{ \AA}$ ,  $\angle C\text{--}H\cdots O = 104.6\text{--}119.6^\circ$ ). Although the individual interactions are not so strong, two H-bonding interactions from each pyridine molecule function cooperatively with the M–N coordinate bond. With respect to intercage interactions, individual cages of **1** do not align. Rather, the packing optimizes  $C\text{--}H\cdots O$  interactions between the two noncoordinating sulfonate oxygen atoms and the ligated pyridine molecules of adjacent cages ( $H\cdots O = 2.320\text{--}2.378\text{ \AA}$ ,  $\angle C\text{--}H\cdots O = 160.9\text{--}174.2^\circ$ ). Twelve such interactions are formed between each cage and its neighbors. Aside from the guest pyridine inside the cage, there are no other included molecules in compound **1**, including the intercage spaces.

**Single-Crystal Structure of Compound 2.** The structure of compound **2** resembles 1-D ladders where each set of rungs is formed by a 4:4 assembly of L molecules and  $[Cu\text{--}(py)_4]^{2+}$  units as shown in Figure 3a. This compound differs from **1** only by the degree of noncoordinated solvent and would be a pseudopolymorph of **1**. Both the spacing between individual rungs of the ladder,  $17.59(2)\text{ \AA}$ , and the breadth of the ladder,  $25.91(2)\text{ \AA}$ , are defined by the transannular Cu–Cu distances. The cavity within the rings of the ladder

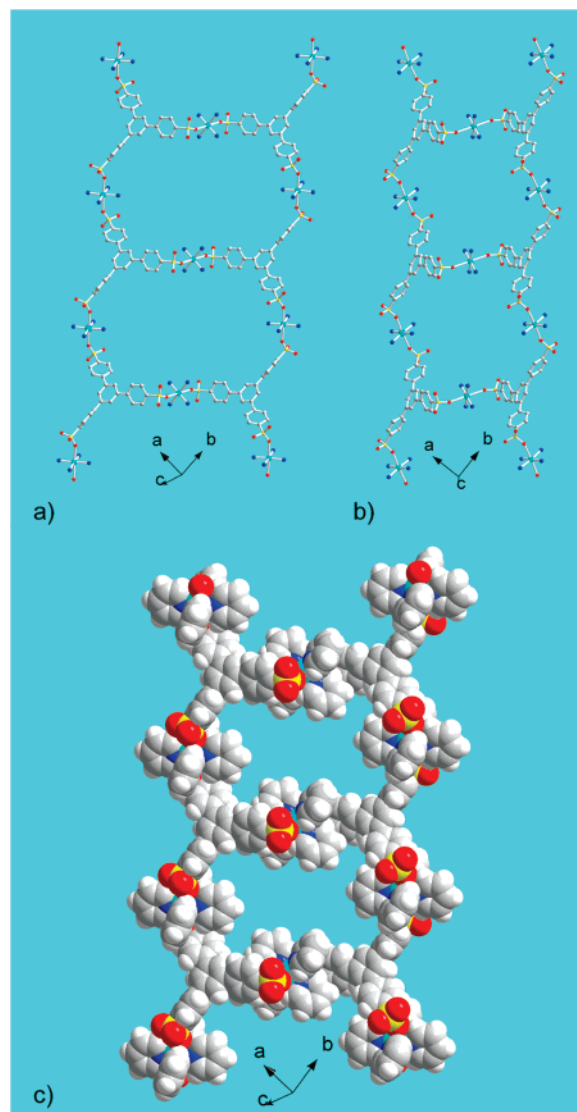


**Figure 3.** Single-crystal structure of compound **2**. For (a) and (b), for pyridine only the N atoms are shown. (a) View of the ladder structure with guest solvent deleted. (b) Rotated view of the ladder to show the nonplanarity of the structure required by the *trans*-sulfonate ligated Cu centers. (c) Space-filling rendition of a single ladder. Pyridyl groups of adjacent ladders fill much of the cavity.

in **2** is more X-shaped in nature due to the ligated pyridine groups. The geometry at each of the two crystallographically unique Cu centers is again Jahn–Teller distorted with the sulfonate groups in the axial positions ( $Cu1\text{--}N = 2.023(7)\text{--}2.112(9)\text{ \AA}$ ,  $Cu1\text{--}O = 2.525\text{--}2.558(8)\text{ \AA}$ ,  $Cu2\text{--}N = 1.899(6)\text{--}2.163(8)\text{ \AA}$ ,  $Cu2\text{--}O = 2.494(8)\text{ \AA}$ ) with the sulfonate oxygen atoms coordinated axially ( $Cu\text{--}O2 = 2.461(3)\text{ \AA}$ ). Each ladder is not perfectly flat, as the axial ligation of the sulfonate groups at the Cu centers enforces two kinks in the rings per Cu site as shown in Figure 3b. The extent of this kinking at each Cu center is  $102.0(2)^\circ$ ,  $104.5(2)^\circ$ , and  $123.8(2)^\circ$  on the basis of the angle between the Cu center, the sulfonate S atom, and the S-bound carbon atom of L. This results in lateral offsets between sequential molecules of L in the rings of  $7.728(9)$  and  $7.775(9)\text{ \AA}$  for the ligands axially bound to Cu1 and Cu2 sites, respectively.

By looking at the extended structure of **2**, it can be observed that adjacent ladders do not align. Rather, they are

offset by half the length of the diagonal of the  $a$  and  $b$  axes, a value equal to 11.81(1) Å. This offset alignment enables the pyridyl ligands of  $[\text{Cu}(\text{py})_4]^{2+}$  units in an adjacent ladder to protrude into a given ladder and to create less void space. The packing between adjacent ladders both laterally and on top of one another is not highly efficient. This is manifested both as the inclusion of two additional molecules of guest pyridine per formula unit and as disorder in the ligated pyridine molecules. On Cu1, two of the four crystallographically inequivalent pyridine ligands are disordered by a partial rotation about the Cu–N bond. Similarly, both the crystallographically unique types of pyridine ligand (i.e., all four ligands) on Cu2 are disordered about the Cu–N bond. To the sides of a given ladder, as oriented in Figure 3a, no components of the next adjacent ladder have any contacts with the first ladder shorter than 3.9 Å. Between adjacent ladders, one guest molecule of pyridine is situated. This molecule has no contacts with adjacent L molecules and pyridine ligands shorter than 3.7 Å. The second type of pyridine guest is located between the rungs of the ladder in the proximity of the Cu2 centers. It forms van der Waals contacts (3.7–3.8 Å) with two Cu2-ligated pyridine molecules as well as the phenyl groups of two molecules of L from adjacent ladders.

**Single-Crystal Structure of Compound 3.** Compound 3 differs from 1 and 2 in that one of the three sulfonic groups is protonated. The presence of one  $\text{SO}_3\text{H}$  group on each molecule of L necessitates a different stoichiometry for the overall solid, so 3 is not a polymorph of 1 or 2. Compound 3 possesses several levels of complexity with respect to its structure. The first level of assembly of the solid can be regarded as the formation of 1-D ribbons, as shown in Figure 4a, that lie along the diagonal of the  $a$  and  $c$  axes. The ribbons are composed of  $[\text{Cu}(\text{py})_4]^{2+}$  units linked by molecules of  $\text{HL}^{2-}$  alternating to either side of the ribbon. Interestingly, as will be discussed later, this compound is likely an intermediate in the formation of compound 2. As in 2, the Cu centers induce kinks in the ribbons. The coordination sphere of the Cu centers is again a tetragonally elongated six-coordinate geometry where one Cu–O distance is significantly longer than the other (Cu–N = 2.015(7)–2.039(9) Å, Cu–O21 = 2.653(9) Å, Cu–O33 = 2.378(8) Å).

The next level of complexity in the structure of 3 is the alignment of 1-D ribbons to form 2-D layers. This is shown in parts b and c of Figure 4 where a single ribbon is highlighted in pink. The plane of the Cu atoms defines the central plane of the layer. Adjacent ribbons project to opposite sides of a layer, and between ribbons within a layer, there are no significant interactions. The shortest H···H distance, along the  $c$  direction, is 6.93(2) Å. Although not so apparent from Figure 4, this value is enforced by the mismatch in the breadths of  $[\text{Cu}(\text{py})_4]^{2+}$  units, the equatorial planes of which largely comprise the layer, and the much narrower pendent molecules of HL. This relationship is more visible in Figure 5a. Also from Figure 4b, it may appear as though, projecting back along the  $a$  direction, the pendent aryl rings of L are  $\pi$  stacked. In fact, adjacent phenyl groups

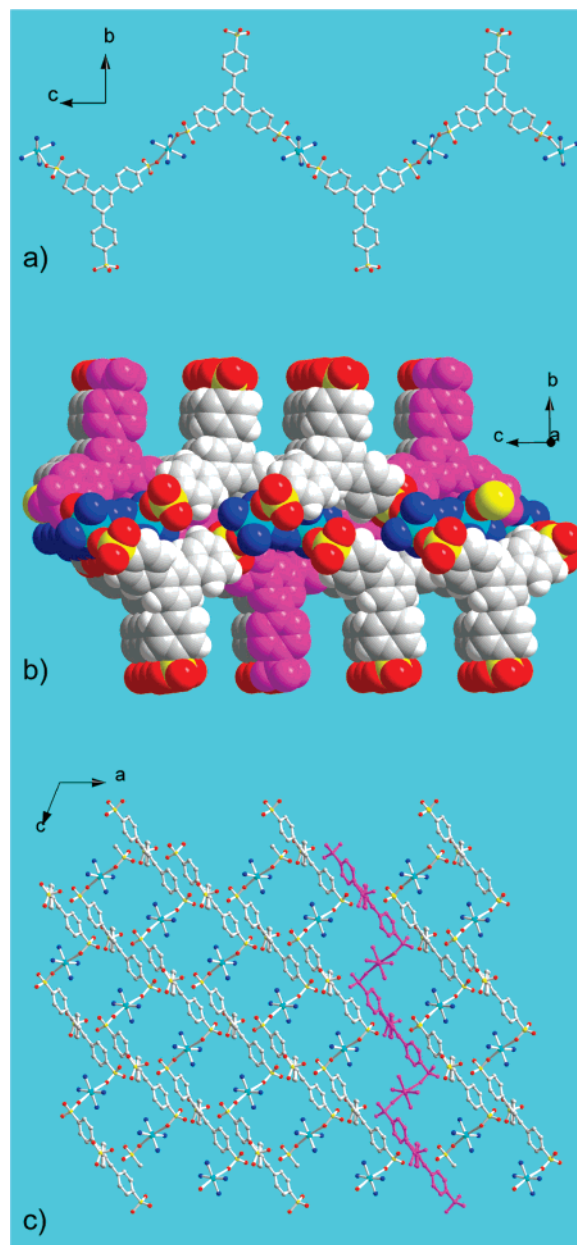


**Figure 4.** Crystal structure of 3. For pyridine, only the N atoms are shown. (a) View of a single ribbon with free  $\text{SO}_3\text{H}$  groups. Views down (b) the  $a$  axis in space-filling mode and (c) the  $b$  axis, which shows the packing of ribbons into layers. One ribbon is shown in pink.

in this direction have a distance between their  $\pi$  faces of 17.78(2) Å. This distance is enforced simply by the size of the triphenylbenzene core of L.

The final level of structural assembly of 3 is the merging of layers into the third dimension. Figure 5a shows the projection of the pendent molecules of L to one side of the layers of  $[\text{Cu}(\text{py})_4]^{2+}$  units. There are numerous stabilizing interactions between the pyridyl ligands on the Cu centers and the aryl groups of L and between the pyridyl groups on different  $[\text{Cu}(\text{py})_4]^{2+}$  units. These range from 3.7 to 3.9 Å, but none stand out as a particularly efficient intermolecular interaction. As previously noted, there are gaps of  $\sim 6.8$  and 17.8 Å between adjacent protruding aromatic groups. The assembly in the third dimension is achieved by the pendent aromatic groups of one layer interdigitating with the pendent

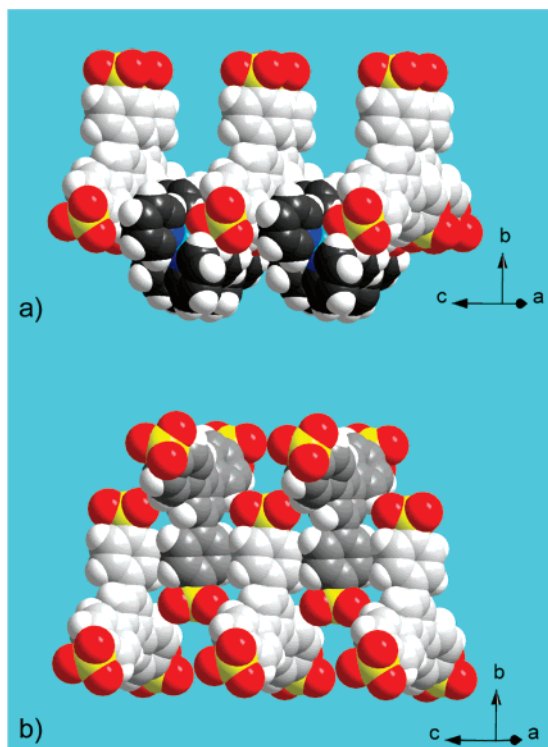


**Figure 5.** (a) Space-filling view of a layer of **3** where the aryl groups of **L** are in light gray and the pyridine rings are in dark gray. (b) View showing the interdigitation of pendent aryl groups from adjacent layers with overlap of their edges to form a 3-D solid.

groups from an adjacent layer. This is much more efficiently realized by filling the  $\sim 6.8$  Å “gaps” in the structure, as shown in Figure 5b, than the larger spacings. A 6.8 Å space is smaller than ideal for accommodating an aromatic by  $\pi$ -stacking interactions (typically 7.0–7.5 Å). As such, the aryl groups align on a skewed axis where only the edges of aryl rings overlap ( $C\cdots C = 3.157\text{--}3.169(7)$  Å). The most remarkable aspect of the structure of **3** is the net result of the interdigitation of adjacent layers to form the open structure shown in Figure 6. Figure 6 shows large open channels that permeate compound **3** down the *c* axis. The lateral breadth of the channel, from left to right as shown, is 16.6(1) Å. Vertically, the channels are 14.8(1) Å high. The channels are occupied by several guest-solvent molecules. In contrast to compound **2**, where pyridine ligands from adjacent ladders fill much of the void space, the channels in **3** as depicted in Figure 6 are filled only with guest solvent. Two crystallographically unique guest molecules of pyridine were located and refined in the single-crystal structure, and numerous additional residual positions were assigned to disordered water molecules.

**Single-Crystal Structure of Compound 4.** Compound **4**, such as compound **3**, contains one protonated sulfonate group, and the ligand is present as a dianion. The structure of **4** is remarkably similar to that of **3**. Compound **4**, at the lowest level of assembly, is composed of tetragonally elongated  $[\text{Cu}(\text{py})_4]^{2+}$  units which are linked, via axial ligation of sulfonate groups of  $\text{HL}^{2-}$ , into 1-D ribbons. The coordination spheres of the two crystallographically unique Cu centers, as in **1–3**, are again Jahn–Teller distorted octahedra

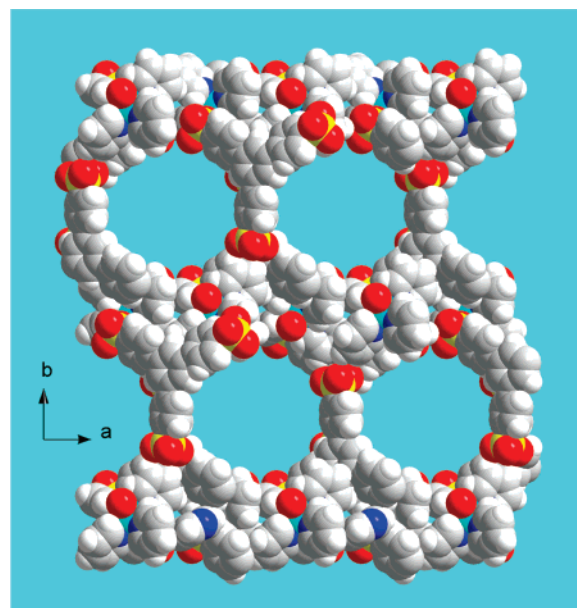


**Figure 6.** Space-filling representation of compound **3**, showing the open channels, formed from the interdigitation of layers, that permeate the solid down the *c* axis. The dimensions of the channels are  $\sim 14.8$  Å high  $\times$  16.6 Å wide.

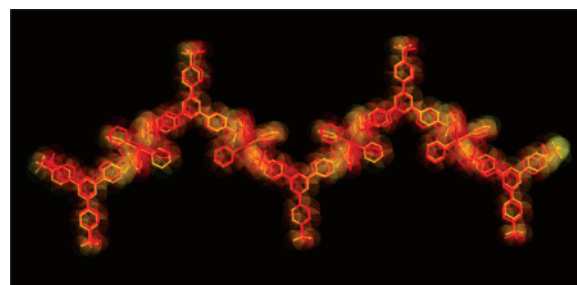


**Figure 7.** A comparison of the 1-D ribbon structures of compounds **3** and **4**. Compound **3** is shown in yellow and compound **4** in red. Where only one line appears visible, which is the case for a large part of the figure, the two structures are perfectly overlapped. The main difference between the structures is in the orientation of pyridyl groups.

( $\text{Cu–N} = 2.016(5)\text{--}2.038(5)$  Å,  $\text{Cu–O} = 2.414\text{--}2.545(4)$  Å). The higher orders of assembly for **4** are exactly as in those of **3** in that ribbons align to form layers and layers subsequently interdigitate to form open channels. Figure 7 shows an overlaid view comparing the structures of the 1-D ribbons formed by compounds **3** and **4**. Clearly, the structural relation is very close, although the exact orientations of each coordinated pyridyl group differ slightly. In **4**, as in **3**, the primary interactions sustaining an individual layer are van der Waals interactions between pyridyl groups and between pyridyl groups and **L** molecules ( $C\cdots C = 3.8\text{--}4.0$  Å). The final level of assembly involves the interdigitation of pendent aryl moieties to form channels as shown in Figure 8. The channels in **4** are more circular than those in **3** having dimensions of  $\sim 16.7 \times 16.7$  Å. The channels are filled with a mix of ordered and disordered water molecules, 2.25 per copper center, as modeled crystallographically. The interdigitated aryl groups overlap at their edges to define the walls of the channels with the shortest  $C\cdots C$  distances of 3.285(8)–3.322(8) Å. A quick comparison of Figure 8 to Figure 6 shows the obvious structural similarity between compounds **3** and **4**.

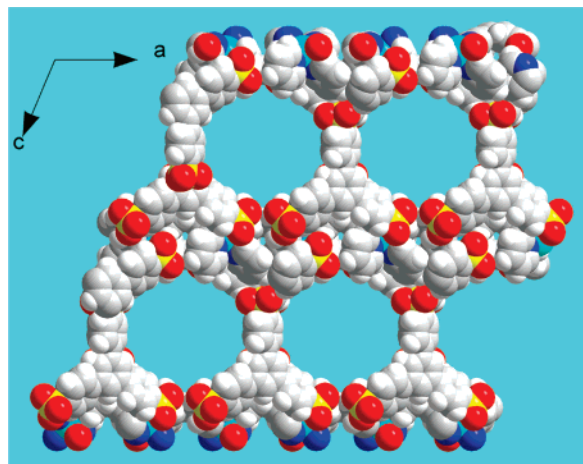


**Figure 8.** Space-filling representation of compound **4**, showing the open channels down the *b* axis. The dimensions of the channels are  $\sim 16.7$  Å high  $\times$  16.7 Å wide. Guest water molecules have been removed.

**Stability of Networks 1–4.** The stability of any network architecture, whether in regard to the process of guest removal or guest exchange, is an important consideration for any functional network material. The three networks presented, for different reasons, are not functional in this regard. For compound **1**, the network stability and the exchangeability of the included guest in the complex were examined. TGA data revealed the solid to be stable to 125 °C, from which point up to 325 °C the pyridine ligands and guest are lost in three steps. More interesting is the resistance of the guest pyridine to exchange. Crystals of complex **1** were heated in toluene-*d*<sub>7</sub> at 100 °C. After 20 h, the <sup>1</sup>H NMR spectrum showed no trace of either pyridine or ligand **L** in solution. A space-filling model of the structure (see Supporting Information) clearly demonstrates the degree to which the guest pyridine is contained and isolated from the exterior of the cage. Given the labile nature of the ligated pyridine molecules, the efficient encapsulation of the guest pyridine, on its own, seemed an insufficient explanation to explain the inertness of the guest with respect to exchange. The guest is locked in place by the ligated pyridine units, and anything which would augment their stability would increase the inexchangeability of the guest. Additional H bonds are formed between the  $\alpha$ -Hs of the ligated pyridine molecules and the axially coordinated sulfonate O atom ( $O \cdots H = 2.567\text{--}2.940$  Å,  $\angle C\text{--}H \cdots O = 104.6\text{--}119.6^\circ$ ). Upon examination of the intermolecular packing of cage molecules, additional C–H $\cdots$ O interactions between the two noncoordinating sulfonate oxygen atoms and the pyridine ligands of adjacent cages ( $H \cdots O = 2.320\text{--}2.378$  Å,  $\angle C\text{--}H \cdots O = 160.9\text{--}174.2^\circ$ ) are observed. Twelve such interactions are formed between each cage and its neighbors. Collectively, these weaker H bonds play a role in augmenting the stability of both the coordinated and, hence, guest pyridine molecules. Compounds **2** and **3** both readily desolvate with a concurrent loss of crystallinity. The fact that **2** and **3** can only be isolated by mechanical separation from the mixture shown in Figure 1 coupled with their rapid desolvation renders essentially impossible the extraction of a sample on which meaningful thermal analysis data could be obtained, and this data is not provided for these

compounds. However, it can be safely stated that neither solid has any notable robustness. This was affirmed by TGA analysis on **4**. Sufficient crystalline material for analysis was readily attainable, as **4** is the sole product in its crystallization. TGA analysis of **4** showed an immediate and continual mass loss from room temperature to 425 °C corresponding to loss of guest water molecules and ligated pyridine.

## Discussion

A crystalline network solid represents the optimized summation of a vast number of intermolecular interactions. A question that is omnipresent in the discussion of any coordination network is that of design, as even the most thoughtful strategies can yield unpredicted structures. This issue is compounded for the preparation of a network solid with open channels, as the enthalpic gain of matching favorable interactions is often more than countered by the energetic penalty of forming a pore. The net result is that often multiple crystalline forms of structurally related compounds have been reported, including polymorphs, pseudopolymorphs, or supramolecular isomers, typically brought about by a change in the preparative conditions (solvent, counterion, pH).<sup>3</sup> The present work exemplifies the subtleties in designing coordination networks as three structurally related compounds result from the same crystallization, a discrete cage, **1**, an open-channel ladder compound, **2**, and a 1-D ribbon that assembles into large open channels, **3**. Compound **3** is particularly interesting in that it is likely an intermediate in the formation of **2** and it offers insights into the design of open-pore structures from 1-D building blocks. Finally, compound **4**, prepared by a different route, represents essentially a high-yield preparation of a motif analogous to compound **3**.

The relative yields of the product solids **1–3** can be varied by the choice of counteranion. With ClO<sub>4</sub><sup>−</sup>, compound **1** can be obtained as the exclusive product. With BF<sub>4</sub><sup>−</sup>, compounds **1** and **2** are obtained in a 98:2 ratio. In the case of nitrate or sulfate, all three compounds are obtained in an approximate 1/2/3 ratio of 90:9:1. In both cases, these yields are approximate and estimated optically on the basis of the different crystalline habits of the three compounds. Figure 1 shows the outcome of a typical recrystallization and the distribution of the three different crystal habits throughout. Powder X-ray diffraction (PXRD) analysis of a bulk precipitate of the nitrate salt showed primarily compound **1**, paralleling the single-crystal growth (see Supporting Information). Additional broad peaks were observed where peaks for compounds **2** and **3** would be expected, on the basis of comparison to the simulated PXRD of the crystals. These are attributed to desolvated **2** and **3**, which lose crystallinity upon removal from the mother liquor. Regardless of the choice of counterion, the addition of small amounts of methanol to the aqueous crystallization results in the exclusive formation of **1**. The addition of a small amount of hexamethylenetetramine results in the exclusive formation of **4**, structurally very similar to **3**. Different network structures can be obtained from identical building blocks, that is, the observation of supramolecular isomers. However,

when observed, these are typically formed under different conditions, albeit sometimes only slightly different. In this work, compounds **1** and **2** form at similar rates with **3** forming after the formation of these crystals. This is consistent with a shift in pH of the mother liquor upon crystallization of **1** and **2**, resulting in the formation of **3**. For the formation of **4**, the role of the hexamethylenetetramine is likely as a structural template for the channel rather than as a pH regulator, as its presence would favor deprotonation rather than the presence of  $\text{HL}^{2-}$ .

The observation of three different solids from a single recrystallization is very rare. Concomitant formation of two polymorphs has been observed for molecular species<sup>16</sup> as well as for coordination solids.<sup>17–20</sup> In this particular case, compounds **1** and **2** differ by solvation, so they are not true polymorphs but they do represent supramolecular isomers. Compound **3** has a different stoichiometry owing to the presence of  $\text{HL}^{2-}$ . Kelly et al. have reported the observation of four different crystalline products from the reaction of *S,S'*-diphenylsulfimide with  $\text{CuCl}_2$ .<sup>18</sup> In this work, none of the products are network solids and the primary variation in the compounds is in the geometry and ligation at the Cu coordination sphere. The present work represents quite a contrast in that the overall structural topologies are very different, yet the Cu centers in all three structures are Jahn–Teller distorted geometries with four equatorial pyridine ligands and two axial sulfonate groups. Peresykina et al. have very recently reported that (4-(3',5'-dimethyl-1*H*-pyrazol-1'-yl)-6-methyl-2-phenylpyrimidine)dichlorocopper(II) forms crystals of three different colors.<sup>19</sup> The actual structural features of the complex from each crystal are not markedly different, and the authors attribute the color differences to slight variations in  $\pi$  stacking between coordinated ligands. From a basic design perspective, if one connects trigonal nodes (molecule L) with a linear linker (the *trans*-sulfonate-ligated Cu), the expected structure is typically a honeycomb net. Interestingly, this product is not observed at all in this work.

Compound **3** provides an insight into the mechanism of growth of compound **2** in solution prior to crystallization. Upon examination of the structures of **2** and **3**, a basic difference, aside from the different extended structure, is that in **3** one of the three sulfonate groups is protonated, making the ligand only dianionic. The protonated sulfonic acid group

is the noncoordinating unit and points away from the layer as shown in Figure 4. If the sulfonic acid groups in **3** were deprotonated and the resulting sulfonate groups coordinated axially to  $[\text{Cu}(\text{py})_4]^{2+}$  units, as is the case for each Cu center in **1–3**, the result would be the linking of two ribbons and a structure equivalent to compound **2**. This structural relation indicates that it is likely that **2** is formed from ribbons in solution rather than, for example, the initial formation of rings, which would then link into the ladder structure.

Much of the enormous interest in coordination frameworks and their potential applications hinges on access to the interior of the solid and, hence, open pores in the frameworks. Pores in coordination solids are fundamentally a challenge as the bonding is not as strong as in a metal oxide yet must compensate for the enthalpic cost of creating void space. Arguably, with its large 1-D channels the structure of compounds **3** and **4** could be regarded as the most interesting of those in this work. Unfortunately, neither **3** nor **4** (nor **2**), with their open-channel structures, sustains removal of their guests. That said, the structure of compounds **3** and **4** provides a model for the formation of an open-channel structure from 1-D building blocks. In considering the initial preparation, the low yield of **3** could be interpreted as an indication that this structure was highly disfavored. The formation of **4**, with virtually an identical structure to that of **3**, as the major product employing a template strategy affirms that open channels can be formed in good yield from 1-D building blocks. Furthermore, for both **3** and **4**, it must be considered that these compounds contain a trisulfonated ligand functioning in a dianionic form. With a disulfonate analogue of L, the yields of **3** (and **4**) would be expected to be significantly greater. Indeed, with structurally similar dianionic ligands (e.g., 5-nitro-isophthalic acid), 1-D ribbons have been observed with  $\text{Cu}^{2+}$  as one of two isomeric forms.<sup>20</sup> The key feature in enabling the open-channel structure is the mismatch in the breadth of the backbone of the 1-D polymer, which is defined by the  $[\text{Cu}(\text{py})_4]^{2+}$  units, and the pendent protonated sulfophenyl groups, which are essentially the breadth of an aryl ring. The greater breadth of the  $[\text{Cu}(\text{py})_4]^{2+}$  backbone leaves interdigitation of aryl groups from adjacent layers as the only efficient means of packing the layers even though this necessitates the formation of the open pore. Recall that for **3**, the spacings between pendent aryl groups are  $\sim 6.8$  and  $\sim 17.8$  Å, the smaller gap permitting edge contacts of phenyl rings from different layers. The larger gap then remains to define the open channels. Thus, this steric mismatch offers an interesting prospectus for designing open-channel solids based on 1-D or 2-D structures with pendent groups. Using more strongly ligating bridging groups and less labile ligands on the metal center could then potentially stabilize the solids to permit formation of permanent pores.

## Conclusions

We have presented the very rare observation of three guest-including coordination solids forming from the same crystallization. Compound **1** is a discrete cage with an inexchangeable pyridine guest. Compound **2** is a ladder-type 1-D

- (16) (a) Bernstein, J.; Davey, R. J.; Henck, J. O. *Angew. Chem., Int. Ed.* **1999**, *38*, 3441. (b) Roy, S.; Banerjee, R.; Nangia, A.; Kruger, G. J. *Chem.—Eur. J.* **2006**, *12*, 3777. (c) Kumar, V. S. S.; Pigge, F. C.; Rath, N. P. *New J. Chem.* **2003**, *27*, 1554. (d) Aitipamula, S.; Nangia, A. *Chem. Commun.* **2005**, 3159. (e) Fabian, L.; Kalman, A.; Argay, G.; Bernath, G.; Gyarmati, Z. *C. Chem. Commun.* **2004**, 2114.
- (17) (a) Fromm, K. M.; Doimeadios, J. L. S.; Robin, A. Y. *Chem. Commun.* **2005**, 4548. (b) Braga, D.; Cojazzi, G.; Emiliani, D.; Maini, L.; Polito, M.; Gobetto, R.; Grepioni, F. *CrystEngComm.* **2002**, *4*, 277. (c) Hamamci, S.; Yilmaz, V. T.; Buyukgungor, O. *Acta Crystallogr., Sect. C* **2006**, *62*, M1.
- (18) Holmes, K. E.; Kelly, P. F.; Elsegood, M. R. *J. CrystEngComm.* **2002**, *4*, 545.
- (19) Peresykina, E. V.; Bushuev, M. B.; Virovets, A. V.; Krivopalov, V. P.; Lavrenova, L. G.; Larionov, S. V. *Acta Crystallogr., Sect. B* **2005**, *61*, 164.
- (20) Abourahma, H.; Moulton, B.; Kravtsov, V.; Zaworotko, M. J. *J. Am. Chem. Soc.* **2002**, *124*, 9990.

structure which includes water and pyridine guests. Compound **3** assembles from a 1-D ribbon to layers to its ultimate form of a large open-channel solid. Notably, the metal-coordination sphere in all three compounds is identical, yet three different networks result. In addition to highlighting the subtleties involved in forming network coordination solids, the two infinite frameworks, **2** and **3**, can be related so as to provide an insight to the network growth. By employment of a structure-directing agent in a preparation with identical building blocks, another network, **4**, structurally almost identical to the minor product **3**, can be formed as the sole product solid. The large open frameworks that result in **3** and **4**, although themselves not robust, offer a

paradigm for the construction of porous materials from low-dimensional building blocks.

**Acknowledgment.** The authors thank the Natural Sciences and Engineering Research Council (NSERC) of Canada for support of this research and the Killam Trust for a postdoctoral fellowship to A.H.M.

**Supporting Information Available:** X-ray crystallographic files for compounds **1–4** in a CIF file and PXRD data in a PDF file. This material is available free of charge via the Internet at <http://pubs.acs.org>.

IC0615123